

# The LHC Searches for The Heavy Higgs via Two B-jets plus Di-photon

Ning Chen, Chun Du, Yaquan Fang, Lan-Chun Lü. [arXiv:  
1312.7212].Phys.Rev.D(submitted)

2014.01.24

- 1 Model Building
  - EWSB pattern
  - Type-I and Type-II
  - Parameter space
  - The decay modes of  $H$
  - The productions and signals of  $H$
  - The direct experimental bounds on  $H$
- 2 The Analysis of The  $H \rightarrow hh \rightarrow b\bar{b}\gamma\gamma$  Signals
  - SM background
  - Generator
  - Optimization of kinematic cuts
  - Implications to the LHC searches for  $H$
- 3 Conclusion and Discussion

EWSB pattern:  $SU(2)_L \times U(1)_Y \rightarrow U(1)_{em}$

- SM: a Higgs doublet  $\Phi = \begin{pmatrix} \rho^+ \\ \frac{v+h+i\rho^0}{\sqrt{2}} \end{pmatrix}$

- 2HDM:  $\Phi_1 = \begin{pmatrix} \rho_1^+ \\ \frac{v_1+h_1+i\rho_1^0}{\sqrt{2}} \end{pmatrix}, \quad \Phi_2 = \begin{pmatrix} \rho_2^+ \\ \frac{v_2+h_2+i\rho_2^0}{\sqrt{2}} \end{pmatrix}$

- CP-conserving 2HDM potential with the discrete  $\mathbb{Z}_2$  symmetry of  $\Phi_i \rightarrow -\Phi_i$ .

$$\begin{aligned} V(\Phi_1, \Phi_2) &= m_{11}^2 |\Phi_1|^2 + m_{22}^2 |\Phi_2|^2 \\ &+ \frac{\lambda_1}{2} (\Phi_1^\dagger \Phi_1)^2 + \frac{\lambda_2}{2} (\Phi_2^\dagger \Phi_2)^2 + \lambda_3 |\Phi_1|^2 |\Phi_2|^2 \\ &+ \lambda_4 |\Phi_1^\dagger \Phi_2|^2 + \frac{\lambda_5}{2} \left[ (\Phi_1^\dagger \Phi_2)^2 + h.c. \right]. \end{aligned}$$

- SM: a scalar  $h$ , three Goldstone bosons  $\rho^\pm, \rho^0$

- 2HDM: after rotating to mass eigenstates:

1. Charged Goldstone boson  $\rho^\pm$  and charged Higgs boson  $H^\pm$ .

$$\begin{pmatrix} \rho^\pm \\ H^\pm \end{pmatrix} = \begin{pmatrix} \cos \beta & \sin \beta \\ -\sin \beta & \cos \beta \end{pmatrix} \begin{pmatrix} \rho_1^\pm \\ \rho_2^\pm \end{pmatrix}.$$

2. Pseudoscalar Goldstone boson  $\rho^0$  and pseudoscalar  $A$ .

$$\begin{pmatrix} \rho^0 \\ A \end{pmatrix} = \begin{pmatrix} \cos \beta & \sin \beta \\ -\sin \beta & \cos \beta \end{pmatrix} \begin{pmatrix} \rho_1^0 \\ \rho_2^0 \end{pmatrix},$$

where  $\tan \beta \equiv \frac{v_2}{v_1}$ .

3. Higgs boson  $h$  and  $H$ .

$$\begin{pmatrix} H \\ h \end{pmatrix} = \begin{pmatrix} \cos \alpha & \sin \alpha \\ -\sin \alpha & \cos \alpha \end{pmatrix} \begin{pmatrix} h_1 \\ h_2 \end{pmatrix}.$$

- SM: 2 parameters in Higgs potential

$$V(\Phi) = \frac{1}{2}m_h^2\Phi^\dagger\Phi - \lambda(\Phi^\dagger\Phi)^2,$$

the minimization of this potential gives  $\langle\Phi\rangle = \frac{1}{\sqrt{2}}\begin{pmatrix} 0 \\ v \end{pmatrix}$ , so  $\lambda = m_h^2/2v^2$ , where  $v \equiv 246$  GeV. Just one parameter  $m_h$  as input.

- 2HDM: 7 parameters in Higgs potential  $m_{11}, m_{22}, \lambda_1, \lambda_2, \lambda_3, \lambda_4, \lambda_5$ . After EWSB:  $\langle\Phi_1\rangle = \frac{1}{\sqrt{2}}\begin{pmatrix} 0 \\ v_1 \end{pmatrix}$ ,  $\langle\Phi_2\rangle = \frac{1}{\sqrt{2}}\begin{pmatrix} 0 \\ v_2 \end{pmatrix}$  with  $\sqrt{v_1^2 + v_2^2} = 246$  GeV, there are left 6 free parameters which can be chosen as  $\alpha, \beta$  and 4 Higgs masses  $m_h, m_H, m_A, m_{H^\pm}$ .

- SM:  $\mathcal{L}_{\text{Yukawa}} = -y_\ell \bar{L}_L \Phi \ell_R - y_d \bar{Q}_L \Phi d_R - y_u \bar{Q}_L \tilde{\Phi} u_R + h.c.$
- 2HDM:

$$\mathcal{L}_{\text{Yukawa}} = y_{ij}^1 \bar{\psi}_i \psi_j \Phi_1 + y_{ij}^2 \bar{\psi}_i \psi_j \Phi_2,$$

where  $i, j$  are generation indices. The mass matrix is then

$$M_{ij} = y_{ij}^1 \frac{v_1}{\sqrt{2}} + y_{ij}^2 \frac{v_2}{\sqrt{2}}.$$

To avoid tree level FCNC problem, all fermions with the same quantum numbers (which are thus capable of mixing) couple to the same Higgs doublet.

- $\mathcal{L}_{2\text{HDM-I}} = -y_\ell \bar{L}_L \Phi_2 \ell_R - y_d \bar{Q}_L \Phi_2 d_R - y_u \bar{Q}_L \tilde{\Phi}_2 u_R + h.c.$
- $\mathcal{L}_{2\text{HDM-II}} = -y_\ell \bar{L}_L \Phi_1 \ell_R - y_d \bar{Q}_L \Phi_1 d_R - y_u \bar{Q}_L \tilde{\Phi}_2 u_R + h.c.$
- Rewrite them in SM-like form:

$$\begin{aligned} \mathcal{L}_{\text{Yukawa}}^{2\text{HDM}} = & - \sum_{f=u,d,\ell} \left( \xi_h^f \bar{f} f h + \xi_H^f \bar{f} f H - i \xi_A^f \bar{f} \gamma_5 f A \right) \\ & - \left\{ \frac{\sqrt{2} V_{ud}}{v} \bar{u} (m_u \xi_A^u P_L + m_d \xi_A^d P_R) d H^+ \right. \\ & \left. + \frac{\sqrt{2} m_\ell \xi_A^\ell}{v} \bar{\nu}_L \ell_R H^+ + h.c. \right\}, \end{aligned}$$

where  $P_{L/R}$  are projection operators for left-/right-handed fermions.

# Type-I and Type-II

	Type I	Type II
$\xi_h^u$	$\cos \alpha / \sin \beta$	$\cos \alpha / \sin \beta$
$\xi_h^d$	$\cos \alpha / \sin \beta$	$-\sin \alpha / \cos \beta$
$\xi_h^\ell$	$\cos \alpha / \sin \beta$	$-\sin \alpha / \cos \beta$
$\xi_H^u$	$\sin \alpha / \sin \beta$	$\sin \alpha / \sin \beta$
$\xi_H^d$	$\sin \alpha / \sin \beta$	$\cos \alpha / \cos \beta$
$\xi_H^\ell$	$\sin \alpha / \sin \beta$	$\cos \alpha / \cos \beta$
$\xi_A^u$	$\cot \beta$	$\cot \beta$
$\xi_A^d$	$-\cot \beta$	$\tan \beta$
$\xi_A^\ell$	$-\cot \beta$	$\tan \beta$

- Large  $M_{H^\pm}$  limits: contribution to the  $h$  decay modes through the  $h \rightarrow \gamma\gamma$  triangle loop by charged Higgs bosons  $H^\pm$  is negligible.
- As consistent to the current experimental data, the global fit about the 125 GeV Higgs boson signal strengths on the  $(\alpha, \beta)$  plane pointed to the so-called “alignment limit” where  $c_{\beta-\alpha} \rightarrow 0$ . Consequently, one has  $g_{hVV} \rightarrow g_{hVV}^{(\text{SM})}$  and  $g_{hff} \rightarrow g_{hff}^{(\text{SM})}$  under this limit. In our analysis, we often take the following alignment parameter sets:

$$2\text{HDM} - \text{I} : c_{\beta-\alpha} = 0.4, \quad 2\text{HDM} - \text{II} : c_{\beta-\alpha} = -0.02,$$

and vary  $t_\beta \in (1, 10)$ .

- we fix two other input parameters of  $M_A = 600$  GeV and  $\lambda_5 = -6$  subject to the Higgs potential stability constraints.

# The decay branching ratios of $H$

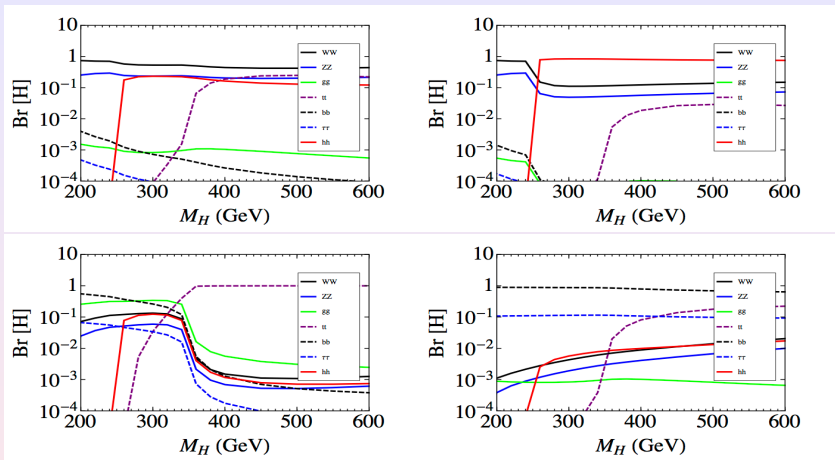


Figure : The decay branching ratios of  $H$  in the mass range of  $M_H \in (200, 600)$  GeV. *Upper left:* 2HDM-I ( $t_\beta = 1$ ), *upper right:* 2HDM-I ( $t_\beta = 10$ ), *lower left:* 2HDM-II ( $t_\beta = 1$ ), *lower right:* 2HDM-II ( $t_\beta = 10$ ).

# The productions of $H$

$H$  can be produced via channels of: (i) the gluon fusion, (ii) the vector boson fusion, (iii) associated with the vector boson, and (iv) associated with heavy quarks.

For the most dominant gluon fusion process (i), the cross sections are rescaled by:

$$\sigma[gg \rightarrow H]_{(\alpha,\beta)} = \sigma[gg \rightarrow H]_{\text{SM}} \cdot \frac{\Gamma[H \rightarrow gg]_{(\alpha,\beta)}}{\Gamma[H \rightarrow gg]_{\text{SM}}},$$

The production cross sections for  $H$  from channel (ii) and (iii) are highly suppressed by factor of  $\mathcal{O}(10^{-2}) - \mathcal{O}(10^{-4})$  to the corresponding SM cases when taking the alignment parameter choices.

For the b-quark associated production channels (iv), the relevant processes involve (0, 1, 2) b-quarks in the final states:

$$b\bar{b} \rightarrow H, \quad b/\bar{b}g \rightarrow b/\bar{b}H, \quad q\bar{q}/gg \rightarrow Hb\bar{b}.$$

We also include these cross sections by rescaling from the corresponding SM cases:

$$\frac{\sigma[b\bar{b} \rightarrow H]_{(\alpha,\beta)}}{\sigma[b\bar{b} \rightarrow H]_{\text{SM}}} = \frac{\sigma[b/\bar{b}g \rightarrow b/\bar{b}H]_{(\alpha,\beta)}}{\sigma[b/\bar{b}g \rightarrow b/\bar{b}H]_{\text{SM}}} = \frac{\sigma[pp \rightarrow b\bar{b}H]_{(\alpha,\beta)}}{\sigma[pp \rightarrow b\bar{b}H]_{\text{SM}}} \\ = (\xi_H^d)^2.$$

These b-quark associated cross sections are given by including the NLO QCD corrections. Given that  $\xi_H^d \rightarrow t_\beta$  along with the alignment limit for the 2HDM-II case, it is apparent that the corresponding inclusive cross sections associated with b-quarks in would become sizable.

# Inclusive heavy Higgs production

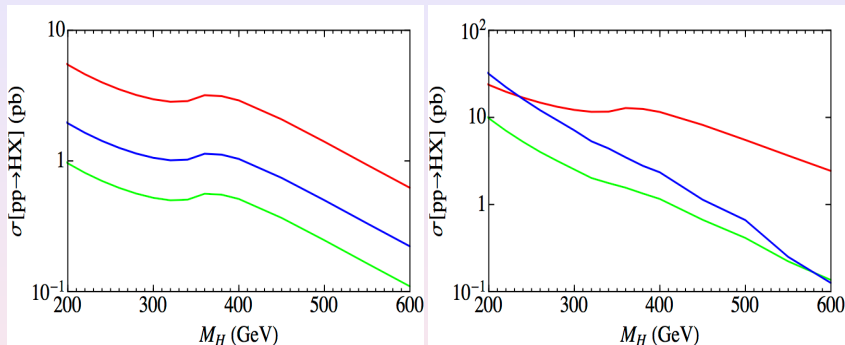


**Figure :** The inclusive heavy Higgs production cross sections  $\sigma[pp \rightarrow HX]$  for  $M_H \in (200, 600)$  GeV: 2HDM-I (left) and 2HDM-II (right) at the LHC 14 TeV run. We show samples with  $t_\beta = 1$  (red),  $t_\beta = 5$  (green), and  $t_\beta = 10$  (blue) for each plot.

# The signals of $H$

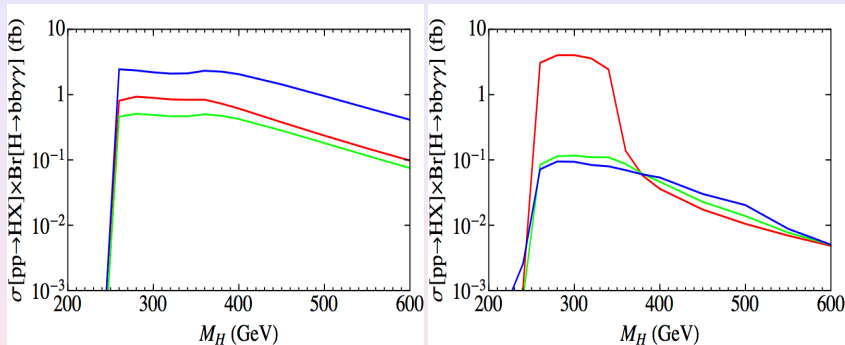


**Figure :** The  $\sigma[pp \rightarrow HX] \times \text{Br}[H \rightarrow hh (h \rightarrow b\bar{b}, h \rightarrow \gamma\gamma)]$  for  $M_H \in (200, 600)$  GeV: 2HDM-I (left) and 2HDM-II (right) at the LHC 14 TeV run. We show samples with  $t_\beta = 1$  (red),  $t_\beta = 5$  (green), and  $t_\beta = 10$  (blue) for each plot.

# The direct experimental bounds on $H$

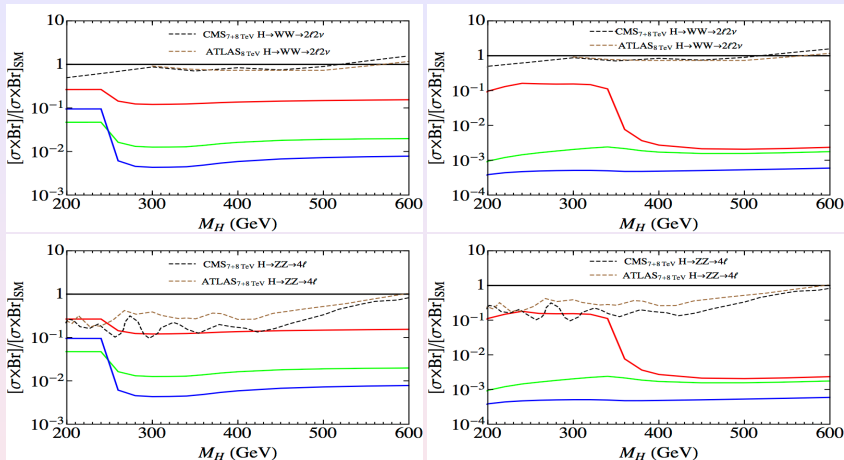


Figure :  $H \rightarrow WW \rightarrow 2\ell 2\nu$  and  $H \rightarrow ZZ \rightarrow 4\ell$  channels for  $M_H \in (200, 600)$  GeV. We demonstrated the exclusions for  $H$  in both 2HDM-I (left panels) and 2HDM-II (right-panels) cases. The inputs of  $t_\beta = 1$  (red),  $t_\beta = 5$  (green), and  $t_\beta = 10$  (blue) are shown.

We analyze the LHC searches for  $H$  via the  $b\bar{b}\gamma\gamma$  final states.

1. The dominant SM background processes include the  $b\bar{b}\gamma\gamma$  and  $t\bar{t}\gamma\gamma$ .

2. Contributions from  $h(\rightarrow \gamma\gamma)Z(\rightarrow b\bar{b})$  and  $h(\rightarrow \gamma\gamma)t\bar{t}$ : negligible.

3. Reducible QCD backgrounds with jets to fake either b-jets and/or photons.

Following the ATLAS detector performance:

- The photon identification efficiencies:

$$\epsilon_{q \rightarrow \gamma} \approx 3.6 \times 10^{-4}, \quad \epsilon_{g \rightarrow \gamma} \approx 3.6 \times 10^{-5},$$

with  $q$  and  $g$  representing the quark-jet and gluon-jet respectively.

- The b-jet mis-tag rates:

$$\epsilon_{c \rightarrow b} \approx 0.2, \quad \epsilon_{j \rightarrow b} \approx 0.01,$$

with  $j$  representing the light jets.

- For the  $b\bar{b}\gamma\gamma$  background, the relevant reducible QCD background contributions include:

$$c\bar{c}\gamma\gamma, \quad j\bar{j}\gamma\gamma, \quad b\bar{b}g\gamma, \quad c\bar{c}g\gamma, \quad j\bar{j}g\gamma, \quad b\bar{b}q\gamma, \quad c\bar{c}q\gamma, \quad j\bar{j}q\gamma, \\ b\bar{b}gg, \quad c\bar{c}gg, \quad j\bar{j}gg, \quad b\bar{b}gq, \quad c\bar{c}gq, \quad j\bar{j}gq, \quad b\bar{b}qq, \quad c\bar{c}qq, \quad j\bar{j}qq;$$

- For the  $t\bar{t}\gamma\gamma$  background, the relevant reducible QCD background contributions include:

$$\bar{t}t\gamma\gamma, \quad \bar{t}tq\gamma, \quad \bar{t}tgg, \quad \bar{t}tgq, \quad \bar{t}tqq.$$

- **FeynRules**: obtain a UFO simplified model containing  $H$  as the only BSM particle. The necessary coupling terms to be implemented include: the cubic  $Hhh$  coupling, the dimension-five  $Hgg$  and  $h\gamma\gamma$  couplings, and the  $H(h)b\bar{b}$  Yukawa couplings.
- **Madgraph/MadEvent**: generate events at the parton level for both signal and background processes.
- **Pythia**: simulating the initial/final state radiation, parton showering, and hadronization.
- **Delphes**: fast detector simulation, where we use the default ATLAS detector card. For the jet clustering, we adopt the anti- $k_T$  jet algorithm with the parameter  $R = 0.6$  for the ATLAS detector card. In addition, we take an overall b-tagging efficiency of 70% for the whole kinematic regions.

- Preliminary cuts by selecting the events with b-jets and photons:

$$n_b \geq 2, \quad n_\gamma = 2.$$

- Cuts on pseudo-rapidities, the transverse momenta, and the mutual  $\eta - \phi$  distances of b-jets and photons:

$$|\eta_{\gamma,b}| < 2.5, \quad p_{T,\gamma} > 25 \text{ GeV}, \quad p_{T,b} > 25 \text{ GeV}, \\ \Delta R(b,b) > 0.4, \quad \Delta R(\gamma,\gamma) > 0.4, \quad \Delta R(b,\gamma) > 0.4.$$

- To reduce the  $t\bar{t}\gamma\gamma$  background, we veto events containing leptons with the transverse momenta of  $p_{T,\ell} > 20 \text{ GeV}$  and the pseudo-rapidities of  $|\eta_\ell| < 2.5$ .

- Cuts on the sum of transverse momenta of the selected b-jets and photons.

For larger  $M_H$  inputs, it is generally more efficient to select events containing hard b-jets and photons.

In practice, we scan over the cuts on the  $p_T$  summations for both heavy Higgs boson signals and the SM background processes in the range of  $\sum_b p_T \in (50, 300)$  GeV and  $\sum_{b,\gamma} p_T \in (100, 600)$  GeV respectively.

Afterwards, the most optimal cuts on  $\sum_b p_T$  and  $\sum_{b,\gamma} p_T$  for each  $M_H$  input are selected by those yielding the largest  $S/B$ .

# Optimization of kinematic cuts

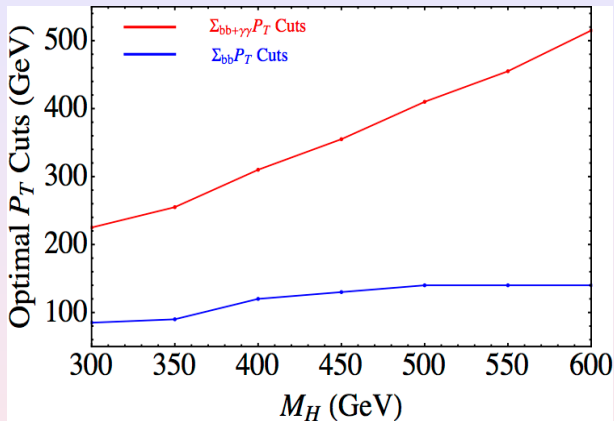


Figure : The most optimal cuts on  $\sum_b p_T$  and  $\sum_{b,\gamma} p_T$  for  $H$  in the mass range of  $M_H \in (300, 600)$  GeV.

- The invariant mass cuts on the selected two b-jets and two photons around the mass window of 125 GeV light Higgs:

$$\begin{aligned} 112.5 \text{ GeV} < m_{bb} < 137.5 \text{ GeV} , \\ 120 \text{ GeV} < m_{\gamma\gamma} < 130 \text{ GeV} . \end{aligned}$$

- For events containing more than two b-jets, we pair all possible combinations and find the one with  $m_{bb}$  mostly close to 125 GeV.

# Optimization of kinematic cuts

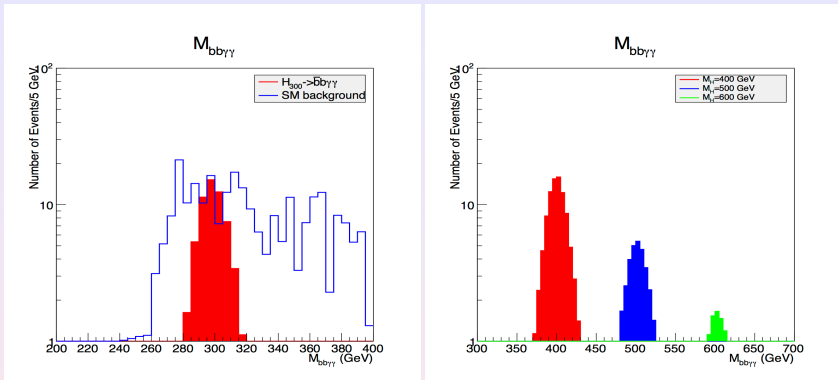


**Figure :** *Left:* The  $m_{bb\gamma\gamma}$  distributions for both signal process with  $M_H = 300$  GeV (red) and background (blue) processes. The nominal cross section of  $\sigma[pp \rightarrow HX] \times \text{Br}[H \rightarrow b\bar{b}\gamma\gamma]$  is taken to be 1 fb. *Right:* The  $m_{bb\gamma\gamma}$  distributions for signal processes with  $M_H = (400, 500, 600)$  GeV. The corresponding signal cross sections are taken for the 2HDM-I with the  $t_\beta = 10$  input. Both plots are evaluated for the LHC 14 TeV run with  $\int \mathcal{L} dt = 1000 \text{ fb}^{-1}$ .

- By observing the  $m_{bb\gamma\gamma}$  distributions for various  $M_H$  inputs, we require the mass window cuts of  $m_{bb\gamma\gamma}$  to be the following:

$$M_H = 300 \text{ GeV} : m_{bb\gamma\gamma} \in (275, 335) \text{ GeV},$$

$$M_H = 350 \text{ GeV} : m_{bb\gamma\gamma} \in (295, 405) \text{ GeV},$$

$$M_H = 400 \text{ GeV} : m_{bb\gamma\gamma} \in (355, 450) \text{ GeV},$$

$$M_H = 450 \text{ GeV} : m_{bb\gamma\gamma} \in (400, 510) \text{ GeV},$$

$$M_H = 500 \text{ GeV} : m_{bb\gamma\gamma} \in (455, 560) \text{ GeV},$$

$$M_H = 550 \text{ GeV} : m_{bb\gamma\gamma} \in (500, 615) \text{ GeV},$$

$$M_H = 600 \text{ GeV} : m_{bb\gamma\gamma} \in (555, 665) \text{ GeV}.$$

By the cut based analysis before, it is straightforward to further look at the LHC search potential to  $H$  via the  $b\bar{b}\gamma\gamma$  final states.

For the LHC discovery, we require the number of signal events after the selection to satisfy  $S \geq \max\{5\sqrt{B}, 10\}$ .

# Implications to the LHC searches for $H$

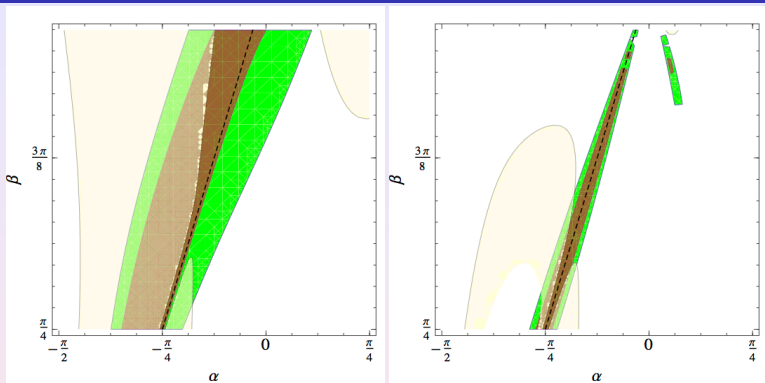


**Figure :** The LHC-14 search sensitivities to the  $H \rightarrow b\bar{b}\gamma\gamma$  final states on the  $(\alpha, \beta)$  parameter space ( $M_H = 300$  GeV case). *left:* 2HDM-I for the  $\int \mathcal{L} dt = 100 \text{ fb}^{-1}$ , *right:* 2HDM-II for the  $\int \mathcal{L} dt = 100 \text{ fb}^{-1}$ . The yellow shadow in each plot represents the parameter regions within the reach via the  $bb\bar{b}\gamma\gamma$  final states. The green and brown bends are the global fit to the 2HDM parameters  $(\alpha, \beta)$  at the 68% and 95% CLs.

# Implications to the LHC searches for $H$

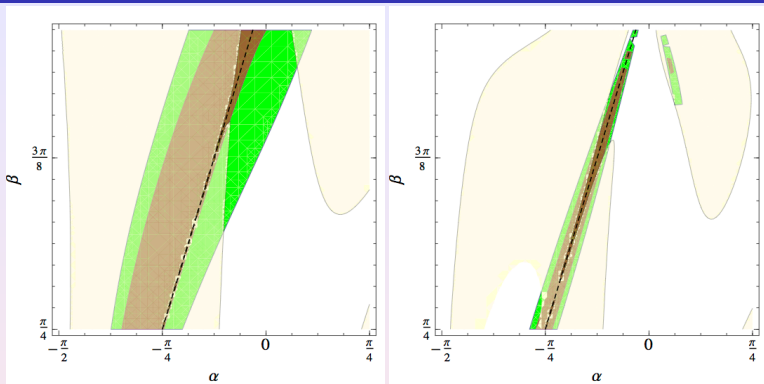


**Figure :** The LHC-14 search sensitivities to the  $H \rightarrow b\bar{b}\gamma\gamma$  final states on the  $(\alpha, \beta)$  parameter space ( $M_H = 300$  GeV case). *left:* 2HDM-I for the  $\int \mathcal{L} dt = 3000 \text{ fb}^{-1}$ , and *right:* 2HDM-II for the  $\int \mathcal{L} dt = 3000 \text{ fb}^{-1}$ . The yellow shadow in each plot represents the parameter regions within the reach via the  $b\bar{b}\gamma\gamma$  final states. The green and brown bends are the global fit to the 2HDM parameters  $(\alpha, \beta)$  at the 68% and 95% CLs.

# Implications to the LHC searches for $H$

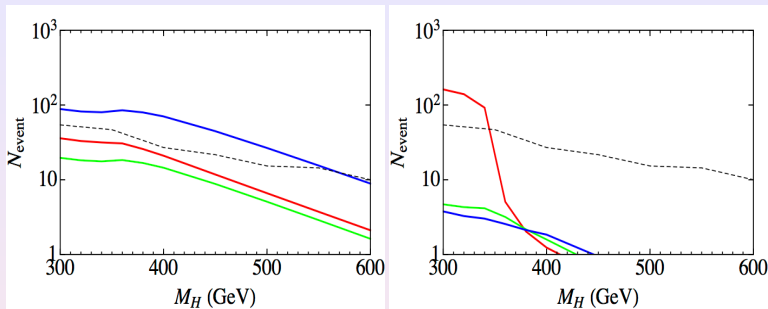


**Figure :** The mass reach of  $H$  via the  $b\bar{b}\gamma\gamma$  final states. *left:* 2HDM-I for the  $\int \mathcal{L} dt = 1000 \text{ fb}^{-1}$ , *right:* 2HDM-II for the  $\int \mathcal{L} dt = 1000 \text{ fb}^{-1}$ . We show samples with  $t_\beta = 1$  (red),  $t_\beta = 5$  (green), and  $t_\beta = 10$  (blue) for each plot. The discovery limit (black dashed curve) of  $\max\{5\sqrt{B}, 10\}$  is demonstrated for each sample with the  $\int \mathcal{L} dt = 1000 \text{ fb}^{-1}$  case.

# Implications to the LHC searches for $H$

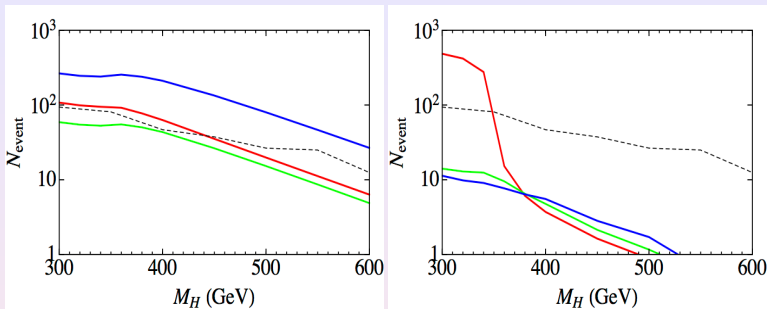


**Figure :** The mass reach of  $H$  via the  $b\bar{b}\gamma\gamma$  final states. *left:* 2HDM-I for the  $\int \mathcal{L} dt = 3000 \text{ fb}^{-1}$ , *right:* 2HDM-II for the  $\int \mathcal{L} dt = 3000 \text{ fb}^{-1}$ . We show samples with  $t_\beta = 1$  (red),  $t_\beta = 5$  (green), and  $t_\beta = 10$  (blue) for each plot. The discovery limit (black dashed curve) of  $\max\{5\sqrt{B}, 10\}$  is demonstrated for each sample with the  $\int \mathcal{L} dt = 3000 \text{ fb}^{-1}$  case.

- In this work, we suggested that the decay channel of a heavy Higgs into two 125 GeV Higgs bosons can be considered as a potentially promising search channel for the upcoming LHC runs at 14 TeV.

- Our discussions are based on the general 2HDM framework, where one is free to set the heavy Higgs boson masses and quartic couplings subject to the theoretical constraints. With proper parameter choices, it is possible to enhance the Higgs cubic coupling term  $\lambda_{Hhh}$ , hence the  $H \rightarrow hh$  decay mode becomes the most dominant one over a broad mass range of  $250 \text{ GeV} \lesssim M_H \lesssim 600 \text{ GeV}$ .

- To search for the final states with two 125 GeV Higgs bosons, we consider the combination of  $b\bar{b}\gamma\gamma$  as our priority.

- By performing the cut-based analysis to different samples of  $M_H$  inputs, we obtain the most optimal cuts and impose them sequentially to both signal and background processes.